Astrometric Measurements and Investigation of Four Double Star Systems

Alexander Castronovo, Tzofia Strey, Mattia Worster, Lerin Alaluf, Kalée Tock

Stanford Online High School, Redwood City, CA; alexandercastronovo@gmail.com

Abstract

This paper investigates the double star systems GLI 16 (WDS 02119-7241), STF 336 (WDS 03015+3225), HWE 20 (WDS 08034-3044), and DAM 1234 (WDS 11380+0319). The position angle and separation values for each system were obtained by taking ten images using Las Cumbres Observatory Global Telescope network 0.4m telescopes. AstroImageJ measurements were plotted alongside other historical data from the Washington Double Star Catalog to determine whether there is a trend. The resulting measurements were analyzed to determine the likelihood that the systems are gravitationally bound. For all four systems, the measured position angle and separation were similar to previous measurements. Our investigation suggests that the four systems whose measurements are presented here are not gravitationally bound, but do have a physical relationship.

1. Introduction

Some early double star observations were recorded by Galileo not to determine if the stars were gravitationally bound, but instead to measure parallax. If the two stars shift relative to each other when the Earth is on the other side of its orbit in 6 months, the closer star's distance from Earth can be determined. William Herschel started measuring the separation and position angles of double stars in 1779 with the same goal as Galileo: to measure parallax. After three years, Herschel found 269 binary stars (Genet et. al, 2012).

Today, finding gravitationally-bound stars is important because it allows the mass of the star system to be estimated from the orbital parameters. The system's mass, in turn, allows astronomers to estimate the masses of stars of a similar spectral type. Plotting the position of the secondary star relative to the primary star over time can reveal a clear orbital path, suggesting a gravitational relationship between the two. However, such a path can sometimes take centuries or millennia to emerge. For the four stars studied here, prior astronomers have not previously identified any orbital patterns.

Table 1 shows known information about the stars studied. The data is collected from Gaia Data Release 3 and the Washington Double Star Catalog.

Table 1. Right Ascension (RA), Declination (Dec) from the Washington Double Star (WDS) catalog, magnitudes of the primary and secondary stars taken from Gaia Gmag, and absolute magnitudes of the primary and secondary stars calculated from the Gaia Gmags and corrected for parallax.

System	RA	Dec	Gaia Gmag Primary	Gaia Gmag Secondary	Gaia Parallax Primary (mas)	Gaia Parallax Secondary (mas)	Absolute Magnitude Primary	Absolute Magnitude Secondary
GLI 16	02:11:55.23	-72:40:44.1	9.56	9.92	5.42	5.39	3.23	3.58
STF 336	03:01:29.07	+32:24:45.8	6.52	8.41	4.13	3.93	-0.4	1.38
HWE 20	08:03:24.53	-30:43:55.8	8.38	10.34	2.64	2.67	0.18	2.47
DAM 1234	11:38:02.48	+03:19:04.6	13.49	13.56	1.61	1.55	4.52	4.51

Note that HWE 20's secondary star is the seventh closest star in the night sky. That star is still chosen as the secondary star because it most closely matches values recorded by prior WDS astronomers, who could not see the closest six stars due to their dimness.

2. Target Selection

Out of the many double star targets that could be studied, these stars were selected because they met certain criteria needed to effectively study the stars using Las Cumbres Observatory Global Telescope (LCOGT) network's 0.4 m telescope in January. Some criteria were also added to increase the likelihood of the system being binary.

The stars need a separation between 5 through 20 arcseconds, so the two stars are as close as possible while still being resolvable by the instruments used. Parallax has to suggest a physical relationship between stars (i.e. parallax with uncertainties overlap or are close to overlapping). The secondary star should have a magnitude less than 13 to ensure that both stars can be observed using the given hardware. Another search criteria is a system whose stars have a difference in magnitude (delta mag) less than 3 to ensure both the primary and secondary stars appear in the same image using the same exposure time and filter. The stars also need to be currently visible in the night sky in order to be imaged. This was done by constraining the RA to 3-13 hours (best RA for optical observing in January). The system also needs to be classified as physical by the Stelle Doppie website (www.stelledoppie.it/), so that the stars have a higher likelihood to be gravitationally bound.

The aforementioned constraints were input into the Stelle Doppie website, which allows a user to filter its double star database from these criteria.

3. Instruments Used

For 3 of the 4 systems, images were taken using the LCOGT network 0.4m SBIG robotic telescope at the Cerro Tololo Observatory in Chile. The images of the remaining system, STF 336, were obtained at the Teide Observatory in Tenerife, Spain. An image of an LCOGT 0.4-meter is shown in Figure 1. These telescopes use a 16-inch RCS tube and 3-element optics C-ring mounting. They have a maximum slewing speed of 10 degrees per second, a tracking accuracy of ~1″, and blind point accuracy of ~30″.

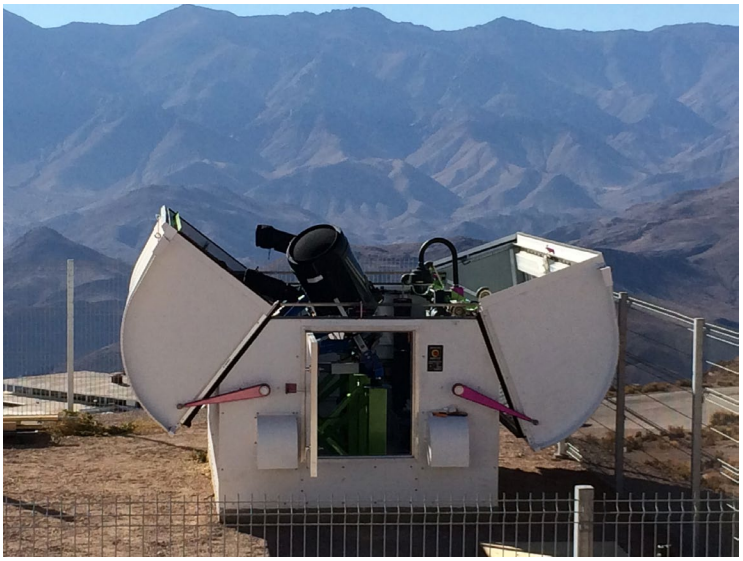

Figure 1. An LCOGT 0.4-meter SBIG robotic telescope in Chile. Image taken by Las Cumbres Observatory.

All double star images in this study were taken using a PanSTARRS-w filter which has a passband of 400 nm – 850 nm, allowing for visible wavelengths of light to be let through. Exposure times were calculated using the following equation, and adjusted if necessary. The only system that needed adjustment was DAM 1234, which used a 60-second exposure instead of 200-second exposure because too much telescope time would be used otherwise, and the 60-second test image was adequately exposed.

(1) $$Exposuretime = 60s \cdot 2.512^{(magnitude-12.5)}$$

This formula ensures that a signal to noise ratio of images taken remains around 250. This formula is derived from the fact that a signal to noise ratio of 250 is present when the exposure time is set to 60 seconds for a 12.5 magnitude star. The exposure time must be multiplied by $2.512^{(magnitude-12.5)}$ because one magnitude lower than any given magnitude is 2.512 times brighter than the original magnitude. Note that this formula ensures a signal to noise ratio of 250 for the visual filter, so it only provides an approximation of the optimal exposure time.

4. Measurement

The AstroImageJ software was used to reduce the LCOGT images of the double star systems. The standard error shown in Table 2 was calculated by taking the standard deviation divided by the square root of 10 (the number of images). The calibrated image files were downloaded directly from LCOGT. Once the images were downloaded, they were checked to make sure that the images were not saturated. Figures 2.1, 2.2, 2.3, and 2.4 show a sample image reduction of each system as well as their corresponding measurement aperture sizes. Tables 2.1, 2.2, 2.3, and 2.4 show the raw data as well as the average and standard deviation from these image reductions.

Figure 2.1. Sample AstroImageJ measurement of the GLI 16 star system using a 5-pixel aperture radius.

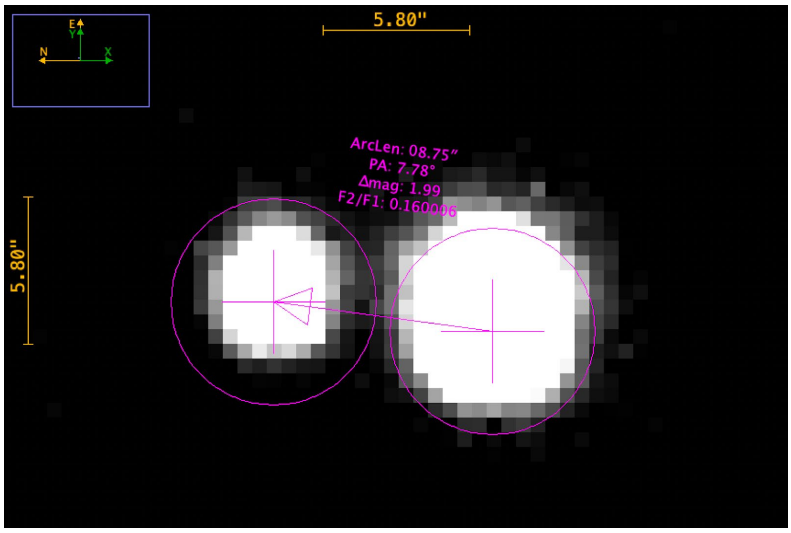

Figure 2.2. Sample AstroImageJ measurement of the STF 336 star system using a 7-pixel aperture radius.

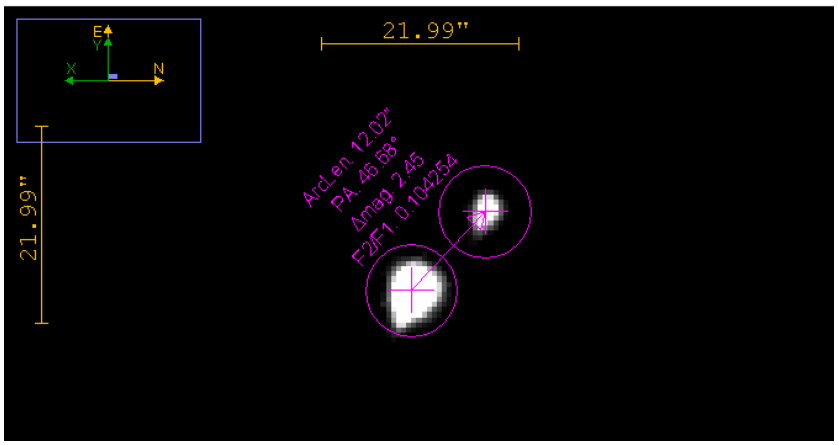

Figure 2.3. Sample AstroImageJ measurement of the HWE 20 star system using a 9-pixel aperture radius.

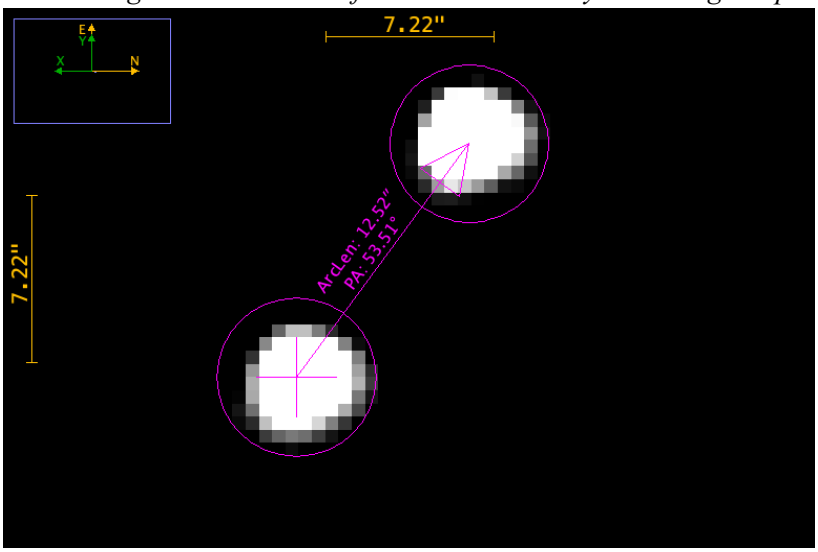

Figure 2.4. Sample AstroImageJ measurement of the DAM 1234 star system using a 6-pixel aperture radius.

Table 2.1. GLI 16 system image reduction data

Image Number	Position Angle (º)	Separation (")
1	160.2	10.4
2	160.2	10.44
3	160.1	10.45
4	160.1	10.39

Table 2.2. STF 336 system image reduction data

Image Number	Position Angle (º)	Separation (")
1	8.1	8.73
2	8.0	8.69
3	7.7	8.76
4	8.2	8.65

5	160.1	10.46
6	160.3	10.49
7	160.0	10.39
8	160.0	10.35
9	160.3	10.37
10	160.2	10.5
Average	160.2	10.42
Standard Error	0.03	0.016

Table 2.3. HWE 20 system image reduction data

5	7.9	8.72
6	7.8	8.67
7	7.7	8.64
8	8.1	8.63
9	7.9	8.67
10	8.0	8.68
Average	7.9	8.68
Standard Error	0.05	0.01

Table 2.4. DAM 1234 system image reduction data

Image Number	Position Angle (º)	Separation (")
1	46.3	12.04
2	46.4	11.86
3	46.6	11.95
4	46.6	11.96
5	46.4	12.01
6	46.2	12.13
7	46.2	12.13
8	46.4	12.05
9	46.8	11.91
10	46.7	12.02
Average	46.4	12.01
Standard Error	0.06	0.028

Image Number	Position Angle (º)	Separation (")
1	55.0	12.71
2	55.1	12.74
3	55.0	12.74
4	55.0	12.73
5	55.1	12.71
6	55.0	12.74
7	55.2	12.78
8	55.2	12.74
9	55.1	12.72
10	55.1	12.73
Average	55.1	12.73
Standard Error	0.03	0.01

5. Formulas

Escape velocity is a useful metric when determining if two stars are binary. If the stars' relative motion is greater than escape velocity, it is impossible for the stars to be in a stable orbit. To find escape velocity, the separation between the two stars must be found. First, we calculate the transverse separation in parsecs using the following formula, where Sep_{angle} is the angular separation in arcseconds, and p is parallax in arcseconds:

(2) $$sep_{transverse} = Sep_{angle} \cdot \frac{1}{3600"} * \frac{1}{p}$$

From the transverse separation, the three-dimensional spatial separation can be estimated using the formula below, where sep_{3D} is the 3D separation in parsecs, Δd is the radial separation (distance of the secondary star from Earth minus distance of the primary star from Earth) of the two stars in parsecs, and $sep_{transverse}$ is the transverse separation of the two stars in parsecs.

(3) $$sep_{3D} = \sqrt{sep_{transverse}^2 + (\Delta d)^2}$$

Finally, we can find a system's escape velocity by using the following formula, where G is the universal gravitational constant in the units $m^3kg^{-1}s^{-2}$, m_1 is the estimated mass of the primary star in kilograms, m_2 is the estimated mass of the secondary star in kilograms, and sep_{3D} is the 3D separation between the primary and secondary stars in meters:

(4) $$v_{esc} = \sqrt{\frac{2G(m_1+m_2)}{sep_{3D}}}$$

The system escape velocity is only useful for determining whether a system is binary if the 3D relative velocity of the stars is also known. First, the relative transverse motion through space must be calculated with the following formula, where tm_{rel} is the relative transverse motion (m/s), PM_{rel} is the relative proper motion with units milliarcseconds (mas) per year and d is distance to the system in parsecs:

(5) $$tm_{rel} = PM_{rel} \cdot \frac{1''}{1000mas} \cdot \frac{1°}{3600''} \cdot \frac{2\pi}{360°} \cdot d \cdot \frac{3.086 \cdot 10^{13} km}{1pc} \cdot \frac{1yr}{3.1536 \cdot 10^7}$$

The relative radial motion through space must also be determined to find the relative 3D velocity. The following formula is used, where rm_{rel} is the relative radial motion, v_1 is the radial velocity of the primary star, and v_2 is the radial velocity of the secondary star:

(6) $$rm_{rel} = v_1 - v_2$$

Finally, the result of these two formulas can be combined to find the 3D relative velocity of the stars. The formula below is used:

(7) $$v_{rel} = \sqrt{tm_{rel}^2 + rm_{rel}^2}$$

Relative 3D velocity and escape velocity for each star can be found in Table 5.

We can infer the mass of the two stars based on their colors and visual absolute magnitudes. The latter is computed from the visual magnitude corrected for parallax according to the following equation, where *m* is the apparent magnitude from Earth, and *p* is parallax in arcseconds:

(8) $$M = m + 5(\log p + 1)$$

The spectral type of each star can be estimated using the color-magnitude diagram (CMD) provided by Gaia seen below in Figure 4 (Babusiaux et al., 2018). The color and absolute magnitude of each star is used to locate the approximate position of the star on the CMD, and this location can then be matched up to the star's spectral type. Subsequently, the mass of each star can be estimated. Either the luminosity of the star is estimated via the HR diagram and converting from Luminosity to mass using this formula:

(9) $$M_{solar} = \sqrt[3.5]{L_{solar}}$$

or by finding the typical mass for a star of its type (Morgan, 2023).

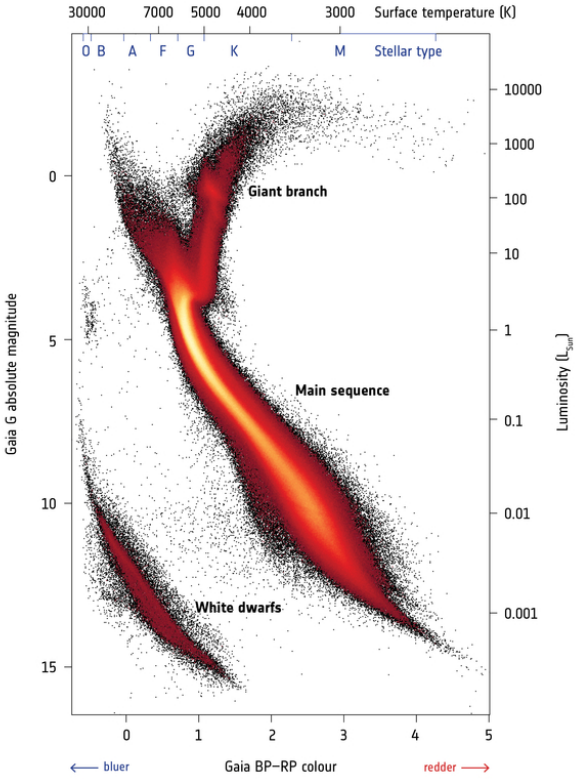

Figure 4. HR diagram from the Gaia Data Release 3 (Vallenari et al., 2022).

6. Results

Below is the data gathered from each of 10 image reductions shown in Table 2.1, 2.2, 2.3, and 2.4 along with their errors.

Table 3. Decimal date of observations, number of images taken using LCOGT telescopes, measured position angle and standard error, measured separation and standard error, and exposure time used for images. DAM 1234's exposure time is set to 60 seconds to not use too much telescope time.

System	Date	Number of Images	Position Angle (°)	Standard error on Position Angle	Separation (Arcsec)	Standard Error on Sep	Exposure Time (sec) *Eq.1*
GLI 16	2023.0166	10	160.2	0.03	10.42	0.016	4.7
STF 336	2023.0466	10	7.9	0.06	8.68	0.013	1.0
HWE 20	2023.0166	10	46.4	0.06	12.01	0.028	1.4
DAM 1234	2023.0419	10	55.1	0.01	12.73	0.002	60.0

The data below, in Tables 4.1 and 4.2, comes from the Gaia mission data release (Prusti et al. and Vallenari et al.) and were found using Stelle Doppie. The rPM is calculated as the ratio of the PM difference vector magnitude to the magnitude of the longer of the component PM vectors (Harshaw, 2016) and is used for classifying pairs as Common Proper Motion. These values are important for calculating the escape velocity of the system (Table 5), which is helpful when determining if the stars are binary.

Table 4.1. Parallax and Gaia Color Information. Uncertainties are also included.

System	Parallax Primary (mas)	Parallax Primary Uncertainty (mas)	Parallax Secondary (mas)	Parallax Secondary Uncertainty (mas)	BP - RP Primary	BP - RP Secondary
GLI 16	5.42	0.049	5.39	0.042	0.59	0.63
STF 336	4.13	0.014	3.93	0.014	1.28	0.51
HWE 20	2.64	0.017	2.67	0.017	1.02	0.52
DAM 1234	1.61	0.030	1.55	0.027	0.79	0.83

Table 4.2. Calculated rPM and proper motion of the primary and secondary stars (Right Ascension, Declination) from the 4 systems including the PM. Uncertainties are also included.

System	Proper Motion Primary (mas/yr) (RA, Dec)	PM Primary Uncertainty (mas/yr) (RA, Dec)	Proper Motion Secondary (mas/yr) (RA, Dec)	PM Secondary Uncertainty (mas/yr) (RA, Dec)	rPM
GLI 16	41.54, 29.96	0.058, 0.046	41.41, 28.98	0.049, -15.47	0.019
STF 336	18.92, -13.96	0.016, 0.018	17.94, -15.47	0.015, 28.98	0.076
HWE 20	-7.20, -0.19	0.020, 0.015	-7.76, 2.63	0.021, 1.79	0.351
DAM 1234	-4.83, 1.99	0.027, 0.033	-5.02, 1.79	0.023, 2.63	0.052

Table 5. Astrometric values calculated from Gaia data in Table 3 according to the formulas outlined in Section 5.

System	Primary Mass (solar masses) *Eq.9*	Secondary Mass (solar masses) *Eq.9*	Primary Star Type *Fig. 4*	Secondary Star Type *Fig. 4*	Escape Velocity (m/s) *Eq. 4*	Relative 3D Velocity (m/s) *Eq. 7*
GLI 16	1.44	1.35	F	F	153	7629
STF 336	2	1.5	Red Giant	A	49	2066
HWE 20	3.7	1.6	Red Giant	A	1431	5473
DAM 1234	1.5	1.5	G	G	30	7922

7. Plots

The values in Table 2 are the raw values from the image reduction. The means of these values are calculated and inserted to Table 3. They are also added to a list alongside all the historical data points. From this, relative RA and Dec is calculated using the formulas below. These formulas are derived knowing that position angle can be represented as the angle of a right triangle, and separation can be represented as the hypotenuse of the right triangle. Declination is negative since the north and south directions are flipped. These data points can be plotted to obtain the values in Figure 3 below.

(10) $$RA = Sep * sin(PA)$$

(11) $$Dec = -Sep * cos(PA)$$

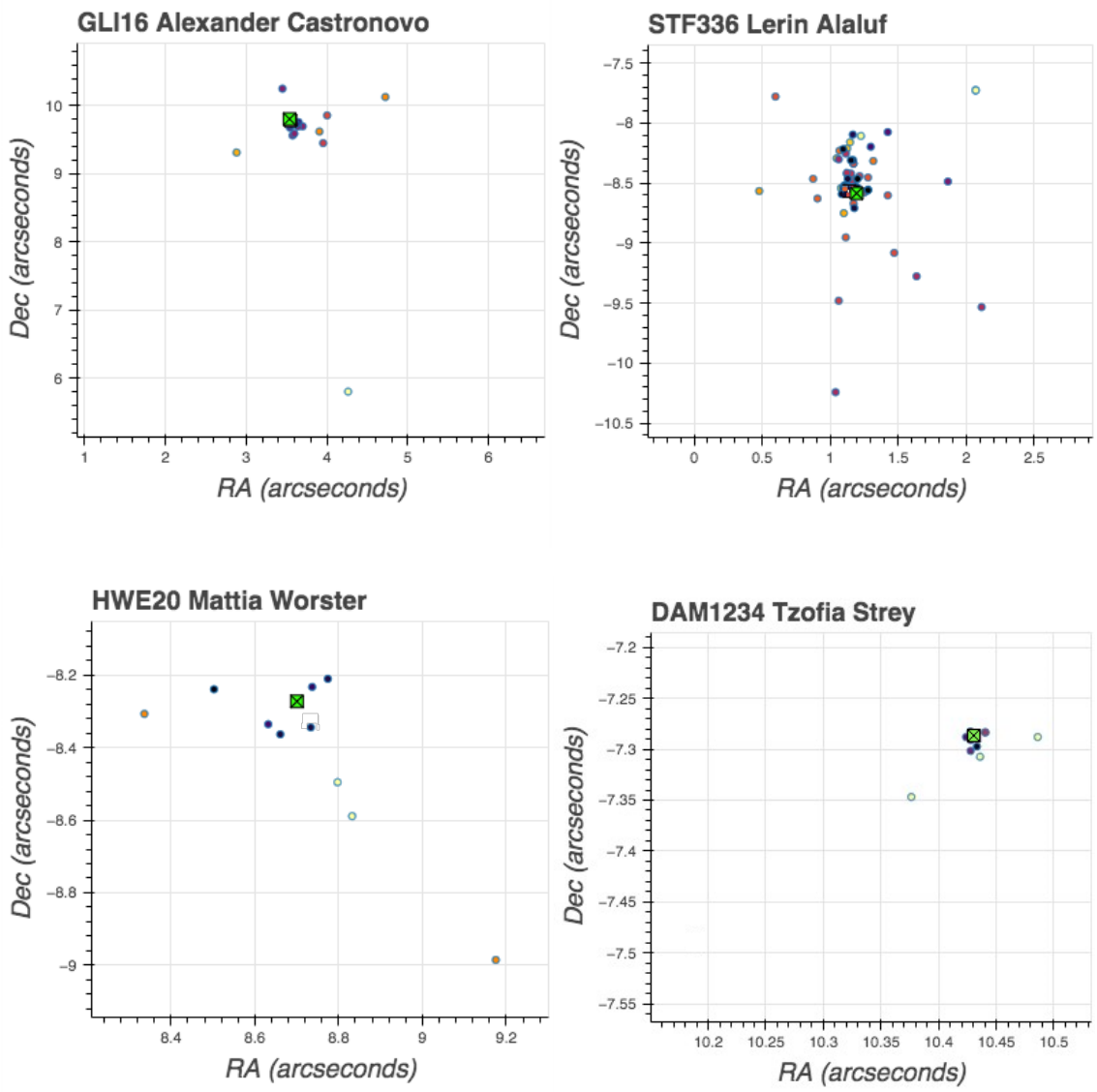

Figure 3. Plots of historical data. Measurements collected in this study are in lime green. Darker points indicate more recent measurements, and lighter points are older measurements. WDS data is used for historical measurements. Coordinates calculated using Eq. 10,11.

8. Discussion

In the case of the double star system GLI 16, both stars appear stationary relative to each other in the transverse dimension as shown in the historical data plot (Figure 3), but the 3D relative velocity in Table 5 suggests that the two stars are moving away from each other. This is possible since the historical data plot only shows transverse separation over time, so the stars might be moving relative to each other on the z axis. Regardless, historical data currently does not currently show indication of an orbit. Additionally, the relative 3D velocity of the double stars greatly exceeds the escape velocity of the system. All of this evidence suggests they are not bound.

The 3D velocity of STF 336 from Table 5 is higher than the system's escape velocity, and it was therefore concluded that the two stars cannot be gravitationally bound. This was further confirmed by the historical data in Figure 3, which showed no curvature, or trend correlating to the time of the measurements. For these reasons, the data suggests that the STF 336 system is a physical double.

The relative 3D velocity (Table 5) of HWE 20's two stars is almost 4 times larger than escape velocity, suggesting that the two stars are not bound. For this reason, the data regarding velocities suggests that the two stars are not gravitationally bound to each other. However, the historical data (which only measures transverse separation) suggests that the proper motion of the two stars is very similar, allowing for the possibility that the two stars' motions are correlated in some way (e.g. expulsion from the same birthplace).

For the DAM 1234 double star system, based on the data obtained from Gaia mission data release and the calculated escape velocity, we can conclude that it is likely that the two stars are not bound. The rPM suggests that the primary and secondary stars have some relationship. However, they are likely not gravitationally bound because the relative 3D velocity (Table 5) of the stars exceeds the escape velocity of the system. So far, the historical data is not evidence enough for an orbit but does support the new measurement made.

9. Conclusion

For all four double stars, the analysis and measurements presented here suggests that none are gravitationally bound. Historical data seems to also support these conclusions. However, based on the measurements from this study and historical measurements, we can conclude that there is a physical relationship between all four stars, making them candidates for continued study in the future. These measurements were conducted as a continuation of Brian Mason's project (Mason, 2020) regarding the observation of double star systems. This paper is our contribution to the important formulation and growth of the Washington Double Star Catalog.

Acknowledgments

This research was made possible by the Washington Double Star catalog maintained by the U.S. Naval Observatory, the Stelle Doppie catalog maintained by Gianluca Sordiglioni (https://www.stelledoppie.it/), Astrometry.net, and AstroImageJ software which was written by Karen Collins and John Kielkopf.

This work has also made use of data from the European Space Agency (ESA) mission Gaia (http://www.cosmos.esa.int/gaia), processed by the Gaia Data Processing and Analysis Consortium (DPAC, http://www.cosmos.esa.int/web/gaia/dpac/consortium). Funding for the DPAC has been provided by national institutions, in particular the institutions participating in the Gaia Multilateral Agreement.

This work makes use of observations taken by the 0.4m telescopes of Las Cumbres Observatory Global Telescope Network located in Tenerife, Spain and Cerro Tololo, Chile.

References

Gaia Collaboration, A. Vallenari, A. G. A. Brown, et al. (2022) Gaia Data Release 3: Summary of the content and survey properties. arXiv e-prints, pp. arXiv:2208.00211.

Gaia Collaboration, C. Babusiaux, F. Van Leeuwen, et al., (2018) Gaia Data Release 2: Observational Hertzsprung-Russell diagrams. A&A 616, A10. https://www.aanda.org/articles/aa/abs/2018/08/aa32843-18/aa32843-18.html

Gaia Collaboration, T. Prusti, J.H.J. de Bruijne, et al. (2016) Gaia Data Release 2: Summary of the contents and survey properties. A&A 595, A1. http://real.mtak.hu/84690/1/gaia6.pdf

Genet, R. M., Fulton, B. J., Bianco, F. B., Martinez, J., Baxter, J. Brewer, M, et al. (2012) Observing double stars. The Society for Astronomical Sciences 31st Annual Symposium on Telescope Science. https://articles.adsabs.harvard.edu//full/2012SASS...31..147G/0000147.000.html

Harshaw, R. (2016) CCD Measurements of 141 Proper Motion Stars. The Autumn 2015 Observing Program at the Brilliant Sky Observatory, Part 3. http://www.jdso.org/volume12/number4/Harshaw_394_399.pdf

Mason, B. (2020) Catalog Access and New List of Neglected Doubles. Journal of Double Star Observations, 16(1), 3-4. http://www.jdso.org/volume16/number3/June_2020_Issue.pdf

Morgan, S. (2023) Spectral Type Characteristics. https://sites.uni.edu/morgans/astro/course/Notes/section2/spectralmasses.html